PROCEEDINGS OF SCIENCE

Λ and Σ potentials in neutron stars, hypernuclei, and heavy-ion collisions

Asanosuke Jinno,[a,*] **Koichi Murase**[b] **and Yasushi Nara**[c]

[a] *Department of Physics, Faculty of Science, Kyoto University, Kyoto, 606-8502, Japan*

[b] *Department of Physics, Tokyo Metropolitan University, Hachioji 192-0397, Japan*

[c] *Akita International University, Yuwa, Akita-city 010-1292, Japan*

E-mail: jinno@ruby.scphys.kyoto-u.ac.jp, murase@tmu.ac.jp, nara@aiu.ac.jp

With an appropriate YNN force, the Λ single-particle potential (Λ potential) can be made strongly repulsive at high density, and one can solve the hyperon puzzle of neutron stars. We investigate the consistency of such a Λ potential, evaluated recently from YN and YNN forces based on chiral effective field theory, with hypernuclear data and heavy-ion collision data. It is found that model calculations with such a Λ potential can reproduce the data of the Λ hypernuclear spectroscopy and the Λ directed flow in heavy-ion collisions. Also, we evaluate the Σ potential, which can be calculated by using the same hyperon forces as for the Λ potential. Specifically, we show that the low-energy constants characterizing the strength of the YNN force can be chosen to suppress the appearance of the Λ's in neutron stars while at the same time the empirical value of the Σ potential is reproduced.

International Conference on Exotic Atoms and Related Topics and Conference on Low Energy Antiprotons (EXA-LEAP2024)
26-30 August 2024
Austrian Academy of Sciences, Vienna.

*Speaker

PoS(EXA-LEAP2024)034

1. Introduction

The hyperon puzzle of neutron stars refers to the observation that most equations of state (EOSs) with hyperons are too soft to support the observed massive neutron stars [1]. One promising solution is that the three-baryon forces (3BFs) among hyperon (Y) and nucleons (N) are strongly repulsive so that the hyperons cannot appear in neutron stars. For example, in Ref. [2], YNN forces have been constructed based on the decuplet dominance approximation [3] and employed together with a YN potential derived within chiral effective field theory (χEFT) [4]. With such a combination, a Λ single-particle potential (Λ potential) fulfilling that scenario can be obtained. A similar Λ potential can be obtained based on the hypernuclear spectroscopy [5]. An analysis employing the up-to-date tuned chiral YN potential [6], which is based on the combined analysis of the $p\Lambda$ scattering and recent $p\Lambda$ femtoscopy data [7], suggests that additional repulsion by the YNN force is required to reproduce the empirical value of the Λ potential at the saturation density.

In this contribution, we examine whether the Λ potentials published in Ref. [2] are consistent with the Λ separation energies of hypernuclei and with the directed flow v_1 of Λ in heavy-ion collisions. Furthermore, we investigate the impact of the YNN interactions proposed in Ref. [2] on the Σ single-particle potential (Σ potential).

Let us emphasize that our work is in line with a recent trend in nuclear matter studies [8–10], conducting a unified approach integrating nuclear experiments and neutron star observations with the modern nuclear force from χEFT to obtain a well-constrained EOS of dense matter. This approach contributes to a more comprehensive understanding of both nuclear experiments and astrophysical observations. For a microscopic description of EOS, the properties of hyperons in nuclear matter should also be constrained. We utilize the experimental data involving hyperons to evaluate the validity of the existing Λ potential, which is important in determining the onset density of strangeness.

2. Evaluating the repulsive Λ potential from Λ hypernuclear data

First, we utilize the Λ hypernuclear spectroscopy to examine the Λ potential. We consider three Λ-potential models (Chi3, Chi2, and LY-IV) as follows (see Ref. [11] for more details): We constructed the Chi3 potential by fitting the result of χEFT with YN and YNN forces [2, 12] to the Skyrme-type Λ potential [11]. The YN force is chosen as NLO13(500) [4], while the YNN force is constructed by the decuplet dominance approximation [3]. For reference, the Chi2 potential was similarly constructed without the 3BF. The LY-IV potential is a conventional Λ potential [13] attractive at high density, with which Λ's appear in dense neutron star matter. The density dependence of the Λ potentials is plotted on the left panel of figure 1. The momentum dependencies for Chi2, Chi3, and LY-IV in the lower momentum region $k \leq 1.0\ \mathrm{fm}^{-1}$ exhibit behaviors similar to those of Kohno2, Kohno3, and LY-IVmomSoft shown on the right panel of figure 1, respectively (see Ref. [11] for the comparison). We employ the Skyrme-Hartee-Fock method using the above-mentioned three different Λ potentials. One parameter that cannot be determined from the uniform-matter results is tuned to reproduce the Λ binding energy data of $^{13}_{\Lambda}\mathrm{C}$.

We compare the model calculations with data on the separation energies of Λ hypernuclei [11] on the left panel of figure 2. Chi3 reproduces the data as accurately as LY-IV. In contrast, we found that Chi2 overbounds by several MeV due to the excessive potential depth at the saturation density $\rho_0 \approx 0.16$ fm^{-3}. Thus, Chi2 can be excluded, yet we need other data to constrain the repulsion of the Λ potential at high densities.

3. Evaluating the repulsive Λ potential from heavy-ion collision data

Next, we consider the rapidity dependence of the Λ directed flow in heavy-ion collisions [15],

$$v_1 = \langle \cos\phi \rangle = \left\langle \frac{p_x}{\sqrt{p_x^2 + p_y^2}} \right\rangle, \tag{1}$$

where ϕ is the azimuthal angle measured from the reaction plane and p_x and p_y are the transverse momenta of a particle. We use the Lorentz vector version of the relativistic quantum molecular dynamics (RQMDv) model [16] implemented in the `JAM2` transport code[1].

In the heavy-ion collision simulation, the high momentum part of the momentum dependence is important. We construct Chi3momSoft, Chi3momHard, and LY-IVmomSoft by extrapolating the momentum dependence of Chi3 and LY-IV to a high momentum region by assuming the Lorentzian form:

$$U_m(\rho(x), k) = \frac{C}{\rho_0} \int d^3k' \frac{f(x, k')}{1 + [(\boldsymbol{k} - \boldsymbol{k}')/\mu]^2}, \tag{2}$$

where C and μ are fitting parameters and $f(x, k)$ is the single-particle distribution function. In the actual heavy-ion simulations, we implement the momentum-dependent potential as the Lorentz

[1] https://gitlab.com/transportmodel/jam2

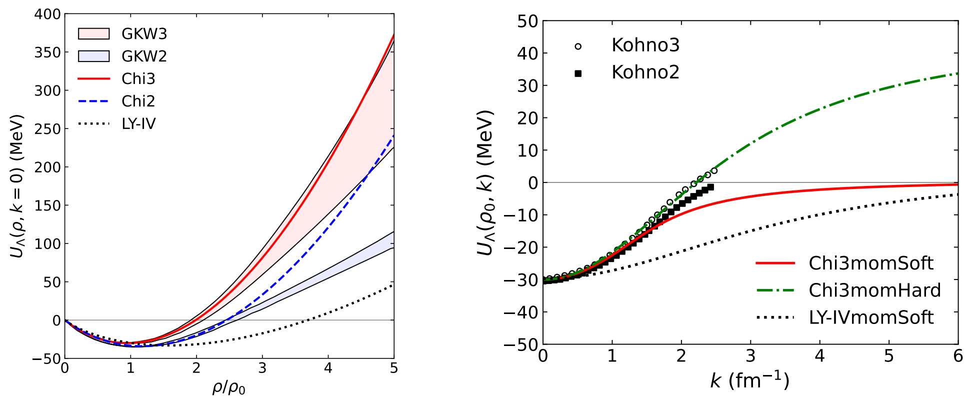

Figure 1: (left panel) Density dependence of the Λ potential. GKW3 represents the results from χEFT with YN and YNN forces [2]. GKW2 is also from χEFT but without the 3BFs [2]. Chi3 (solid line) and Chi2 (dashed line) are fitted to GKW2 and GKW3 up to $\rho/\rho_0 < 1.5$, respectively. LY-IV (dotted line) is a conventional Λ potential [13]. (right panel) Momentum dependence of the Λ potential. Kohno3 represents the result from χEFT with YN and YNN forces [12]. Kohno2 is the result from χEFT without the 3BFs [12]. Chi3momSoft (solid line) and Chi3momHard (dash-dotted line) are constructed to reproduce Kohno3 up to 2.5 fm^{-1} and 1.0 fm^{-1}, respectively. LY-IVmomSoft (dotted line) is fitted to the momentum dependence of LY-IV up to 1.0 fm^{-1}.

vector U^{μ}_{m} [15]. Since χEFT is not entirely reliable above the momentum cutoff of 550 MeV $\simeq$ 2.8 fm^{-1} [12], we prepared two variations: Chi3momHard and Chi3momSoft are constructed to reproduce the χEFT result [12] up to 2.5 fm^{-1} and 1.0 fm^{-1}, respectively. LY-IVmomSoft is constructed to reproduce the momentum dependence of LY-IV with Eq. (2) up to 1.0 fm^{-1}. The momentum dependence of the Λ potentials is plotted on the right panel of figure 1. We note that the density dependence of Chi3momSoft and Chi3momHard is almost identical to that of Chi3, as is LY-IVmomSoft to LY-IV.

The results of v_1 of Λ in mid-central Au + Au collisions at $\sqrt{s_{NN}}$ = 4.5 GeV are shown on the right panel of figure 2 and compared with the STAR data [14]. One can see that both Chi3momSoft and LY-IV reproduce v_1 of Λ with equal accuracy, which implies that v_1 of Λ is not so sensitive to the density dependence of the Λ potential. On the other hand, Chi3momHard underestimates v_1 of Λ, which indicates that v_1 of Λ is sensitive to the momentum dependence of the Λ potential. Experimental information on the optical potential of Λ may be useful for reducing the model uncertainty.

4. How about the Σ potential?

As already mentioned above, in Ref. [2], the 3BFs have been adjusted in such a way that the Λ potential is sufficiently repulsive at high density so that the appearance of Λ hyperons in neutron stars is suppressed. This is possible for different combinations of the low-energy constants (LECs), H_1 and H_2, that characterize the strength of the 3BF (see the solid lines in figure 6 of Ref. [2]). For other combinations, cf. the dashed lines, the repulsion might not be strong enough to achieve that goal.

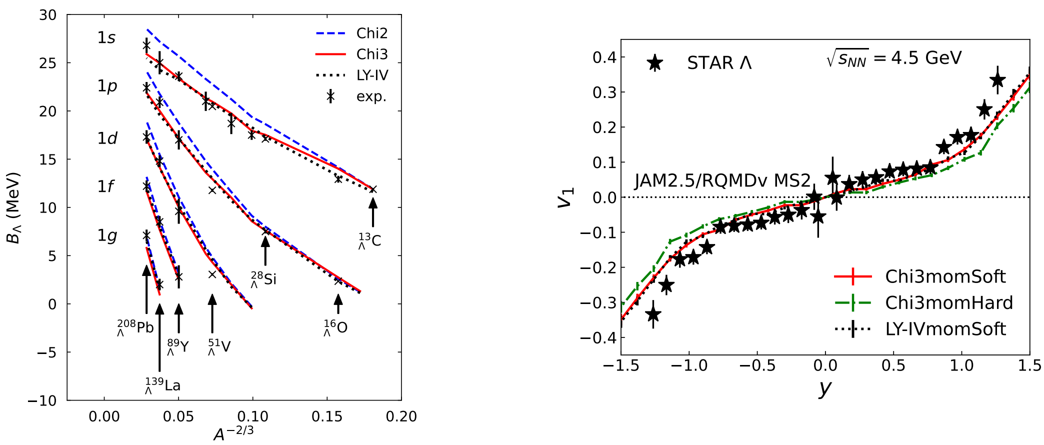

Figure 2: (left panel) Λ binding energy of the Λ hypernuclei. Experimental data (cross) can be found in Ref. [11]. The figure is adopted from Ref. [11]. (right panel) Directed flow of Λ in mid-central Au+Au collisions at $\sqrt{s_{NN}}$ = 4.5 GeV. The STAR data are taken from Ref. [14]. The figure is updated from Ref. [15] by using the updated version of `JAM2`.

H_1 (f^{-2})	H_2 (f^{-2})
−2.650	0.100
−2.200	0.000
−1.800	−0.100
−1.350	−0.200
−0.900	−0.300

Table 1: Considered combinations of LECs of the YNN 3BF that reproduce $U_\Lambda(\rho_0) = -30$ MeV for NLO13(500). The values are in units of the inverse squared pion-decay constant with $f \approx 92$ MeV, and correspond to the left line in figure 6 of Ref. [2]. The values are taken from Gerstung's PhD thesis [21].

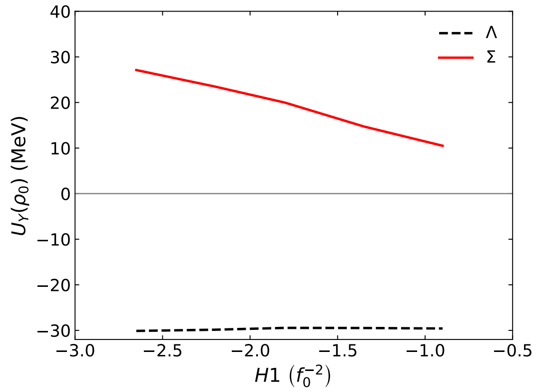

Figure 3: Σ (red solid) and Λ (black dashed) potentials in symmetric nuclear matter. The horizontal axis corresponds to the three-body LECs H_1 with H_2 listed in table 1.

However, it remains unclear how those 3BFs affect the corresponding Σ potential. The effective two-body forces resulting from the 3BFs considered in Ref. [2] contribute not only to the ΛN and ΣN channels but also to the ΛN-ΣN transition potential. A presently accepted constraint on the Σ potential is $U_\Sigma(\rho_0) = 30 \pm 20$ MeV [17], which is inferred using data on Σ^- atoms and on (π^+, K^+) inclusive spectra. This constraint is fairly well met by the original chiral YN potentials from 2013 and 2019 without 3BF [18, 19].

We evaluate the Σ potential in the same way as Gerstung et al. [2] have done for the Λ potential. The Brueckner-Hartree-Fock method with a continuous choice [18] is employed to calculate the hyperon single-particle potential. Regarding the nuclear forces, the N^{3}LO NN potential from Ref. [20] is used, while the NNN 3BF at N^{2}LO is taken into account via a density-dependent two-body force. The cutoff in the regulator function [20] is chosen as 500 MeV. The nuclear saturation properties are reproduced by the nucleon forces [21].

For the hyperonic force, the YN potential NLO13(500) [4] is employed. The YNN force is implemented as an effective density-dependent YN two-body force. The number of LECs involved in the YNN force is reduced by assuming decuplet dominance approximation [3]. Then, there are only three LECs: one related to the meson-octet-decuplet baryon vertex, and two denoted by H_1 and H_2 characterizing the strengths of the contact vertices with three-octet and one-decuplet baryons. The meson-octet-decuplet coupling is constrained by the decay width $\Gamma(\Delta \to N\pi)$, and its large-N_c value is employed [2]. The two LECs of the contact terms are fixed by requiring the reproduction of the empirical value of the Λ potential [11, 17],

$$U_\Lambda(\rho_0) \simeq -30 \text{ MeV}, \tag{3}$$

inferred by using the Λ hypernuclear spectroscopy, and a strongly repulsive U_Λ at high density, sufficient to resolve the hyperon puzzle [2]. Some combinations of the contact LECs that fulfill these requirements are listed in table 1.

The Λ and Σ potentials in symmetric nuclear matter at ρ_0 are shown in figure 3 for various combinations of H_1 and H_2. The Λ potential is practically constant by construction, i.e., due to the

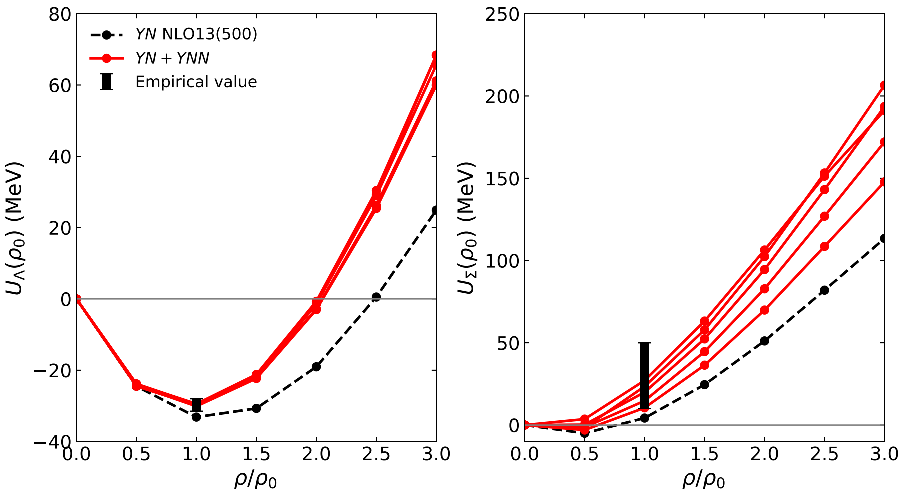

Figure 4: Density dependence of the Λ (left panel) and Σ (right panel) potentials in symmetric nuclear matter. The red solid lines are calculated by using the 3BF LECs in table 1. The only two-body case with the NLO13(500) parameter set is represented by the dashed line. The black bands show the empirical values of the Λ potential, $-31.5 < U_\Lambda(\rho_0) < -28.0$ MeV [11], and the Σ potential, $U_\Sigma(\rho_0) = 30 \pm 20$ MeV [17].

constraint (3). In contrast, the Σ potential varies from about 30 to 10 MeV.

In figure 4, we show the density dependence of the single-particle potentials. One can see that certain sets of the 3BF LECs reproduce the empirical constraint $U_\Sigma(\rho_0) = 30 \pm 20$ MeV [17]. Interestingly, those 3BFs also yield Λ potentials that are strongly repulsive at high densities, as needed to suppress the Λ hyperons in neutron stars. Thus, the 3BFs can be chosen to solve the hyperon puzzle of neutron stars while at the same time the empirical value of U_Σ is reproduced.

5. Summary

To suppress the Λ hyperons in neutron stars, Gerstung et al. [2] calculated the Λ single-particle potential by adding an effective 3BF to the chiral YN potentials of the Jülich-Bonn group [4], which is one of the state-of-the-art modeling of the potential based on the χEFT. In this contribution, we have examined the consistency of those potentials with the data from experiments and observations of substantially different physics. Specifically, we referenced the data from the Λ hypernuclear spectroscopy, the Λ directed flow created in heavy-ion collisions, and the value of the Σ single-particle potential at the saturation density. Some of the 3BF LEC sets of (H_1, H_2) from Ref. [2] turned out to be consistent with the empirical information in all three physics.

The results presented here are based on a single chiral YN potential, NLO13(500). Variants such as NLO19 [19] should be considered in order to provide an estimate of the theoretical uncertainty. Furthermore, recently a YN interaction up to N^{2}LO in the chiral expansion has been presented [22]. Initial studies suggest that it yields more attractive Λ and Σ potentials [22]. Here, a more rigorous investigation of the in-medium properties is required. Such a work will be performed in the future.

In addition, it is desirable to improve the theoretical treatment of the heavy-ion collision simulation. The results shown here have been obtained by using the same Λ potential for all other hyperons, including their resonance states. As a large number of Σ hyperons and hyperon resonances are produced during the evolution of the heavy-ion collisions, and as the behavior of the Λ and Σ potentials are very different, as seen in figure 4, we intend to include different potentials for different hyperons to explore their effects on v_1 of Λ and Σ in future studies.

6. Acknowledgements

AJ thanks Johann Haidenbauer for the collaboration and his careful reading of the manuscript, and Dominik Gerstung for kindly sharing his code with us. AJ also thanks Wolfram Weise and Avraham Gal for insightful and valuable discussions and the nuclear theory group at the Forshungszentrum Jülich for their splendid hospitality during his visit where part of this work was done. This work was supported in part by the Grants-in-Aid for Scientific Research from JSPS (Nos. JP21K03577 and JP23K13102). This work was also supported in part by JST, the establishment of university fellowships towards the creation of science technology innovation, Grant No. JPMJFS2123 and by JST SPRING, Grant Number JPMJSP2110.

References

[1] P. Demorest, T. Pennucci, S. Ransom, M. Roberts and J. Hessels, *Shapiro Delay Measurement of A Two Solar Mass Neutron Star*, *Nature* **467** (2010) 1081 [1010.5788].

[2] D. Gerstung, N. Kaiser and W. Weise, *Hyperon–nucleon three-body forces and strangeness in neutron stars*, *Eur. Phys. J. A* **56** (2020) 175 [2001.10563].

[3] S. Petschauer, J. Haidenbauer, N. Kaiser, U.-G. Meißner and W. Weise, *Density-dependent effective baryon–baryon interaction from chiral three-baryon forces*, *Nucl. Phys. A* **957** (2017) 347 [1607.04307].

[4] J. Haidenbauer, S. Petschauer, N. Kaiser, U.G. Meissner, A. Nogga and W. Weise, *Hyperon-nucleon interaction at next-to-leading order in chiral effective field theory*, *Nucl. Phys. A* **915** (2013) 24 [1304.5339].

[5] E. Friedman and A. Gal, Λ *hypernuclear potentials beyond linear density dependence*, *Nucl. Phys. A* **1039** (2023) 122725 [2306.06973].

[6] D.L. Mihaylov, J. Haidenbauer and V.M. Sarti, *Constraining the p*Λ *interaction from a combined analysis of scattering data and correlation functions*, *Phys. Lett. B* **850** (2024) 138550 [2312.16970].

[7] ALICE collaboration, *Search for a common baryon source in high-multiplicity pp collisions at the LHC*, *Phys. Lett. B* **811** (2020) 135849 [2004.08018].

[8] C. Drischler, J.W. Holt and C. Wellenhofer, *Chiral Effective Field Theory and the High-Density Nuclear Equation of State*, *Ann. Rev. Nucl. Part. Sci.* **71** (2021) 403 [2101.01709].

[9] S. Huth et al., *Constraining Neutron-Star Matter with Microscopic and Macroscopic Collisions*, *Nature* **606** (2022) 276 [2107.06229].

[10] N. Rutherford et al., *Constraining the Dense Matter Equation of State with New NICER Mass–Radius Measurements and New Chiral Effective Field Theory Inputs*, *Astrophys. J. Lett.* **971** (2024) L19 [2407.06790].

[11] A. Jinno, K. Murase, Y. Nara and A. Ohnishi, *Repulsive Λ potentials in dense neutron star matter and binding energy of Λ in hypernuclei*, *Phys. Rev. C* **108** (2023) 065803 [2306.17452].

[12] M. Kohno, *Single-particle potential of the Λ hyperon in nuclear matter with chiral effective field theory NLO interactions including effects of YNN three-baryon interactions*, *Phys. Rev. C* **97** (2018) 035206 [1802.05388].

[13] D.E. Lanskoy and Y. Yamamoto, *Skyrme-Hartree-Fock treatment of Lambda and Lambda Lambda hypernuclei with G-matrix motivated interactions*, *Phys. Rev. C* **55** (1997) 2330.

[14] STAR collaboration, *Flow and interferometry results from Au+Au collisions at $\sqrt{s_{NN}} = 4.5$ GeV*, *Phys. Rev. C* **103** (2021) 034908 [2007.14005].

[15] Y. Nara, A. Jinno, K. Murase and A. Ohnishi, *Directed flow of Λ in high-energy heavy-ion collisions and Λ potential in dense nuclear matter*, *Phys. Rev. C* **106** (2022) 044902 [2208.01297].

[16] Y. Nara and A. Ohnishi, *Mean-field update in the JAM microscopic transport model: Mean-field effects on collective flow in high-energy heavy-ion collisions at sNN=2–20 GeV energies*, *Phys. Rev. C* **105** (2022) 014911 [2109.07594].

[17] A. Gal, E.V. Hungerford and D.J. Millener, *Strangeness in nuclear physics*, *Rev. Mod. Phys.* **88** (2016) 035004 [1605.00557].

[18] S. Petschauer, J. Haidenbauer, N. Kaiser, U.-G. Meißner and W. Weise, *Hyperons in nuclear matter from SU(3) chiral effective field theory*, *Eur. Phys. J. A* **52** (2016) 15 [1507.08808].

[19] J. Haidenbauer, U.G. Meißner and A. Nogga, *Hyperon–nucleon interaction within chiral effective field theory revisited*, *Eur. Phys. J. A* **56** (2020) 91 [1906.11681].

[20] D.R. Entem and R. Machleidt, *Accurate charge dependent nucleon nucleon potential at fourth order of chiral perturbation theory*, *Phys. Rev. C* **68** (2003) 041001 [nucl-th/0304018].

[21] D. Gerstung, *Hyperons in nuclear matter and SU(3) chiral effective field theory*, Ph.D. thesis, Munich, Tech. U., 2020.

[22] J. Haidenbauer, U.-G. Meißner, A. Nogga and H. Le, *Hyperon–nucleon interaction in chiral effective field theory at next-to-next-to-leading order*, *Eur. Phys. J. A* **59** (2023) 63 [2301.00722].